BEST AVAILABLE IMAGES

Defective images within this document are accurate representations of the original documents submitted by the applicant.

Defects in the images may include (but are not limited to):

- BLACK BORDERS
- TEXT CUT OFF AT TOP, BOTTOM OR SIDES
- FADED TEXT
- ILLEGIBLE TEXT
- SKEWED/SLANTED IMAGES
- COLORED PHOTOS
- BLACK OR VERY BLACK AND WHITE DARK PHOTOS
- GRAY SCALE DOCUMENTS

IMAGES ARE BEST AVAILABLE COPY.

As rescanning documents *will not* correct images, please do not report the images to the Image Problem Mailbox.

ELSEVIER

Materials Science and Engineering A231 (1997) 90–97

MATERIALS SCIENCE & ENGINEERING A

Non-stoichiometry and defect structures in rapidly solidified $MgO-Al_2O_3-ZrO_2$ ternary eutectics

Joanna McKittrick [a,*], Gretchen Kalonji [b]

[a] *Department of Applied Mechanics and Engineering Sciences and Materials Science Program, University of California, at San Diego, La Jolla, CA 92093-0411, USA*

[b] *Department of Materials Science and Engineering, University of Washington, Seattle, WA 98195, USA*

Received 18 October 1996; revised 14 January 1997

Abstract

Rapid solidification of the two $MgO-Al_2O_3-ZrO_2$ ternary eutectics was accomplished by inductive heating followed by quenching with a twin roller device. The as-quenched materials exhibited diverse compositional and structural phase assemblages. A metastable binary eutectic between a spinel and zirconia phase was found in the Al_2O_3-rich eutectic composition and had the same composition of the Al_2O_3-rich ternary eutectic. Heat treatment of the samples yielded nucleation of γ-Al_2O_3 and then tetragonal zirconia (t-ZrO_2) at high temperatures as magnesium and oxygen ions diffused from the zirconia phase to the spinel phase. For the as-quenched MgO-rich eutectic, a spinel with nearly the stoichiometric composition formed with cubic-ZrO_2 and MgO. Close to the maximum amount of MgO was dissolved in the spinel and zirconia phases. Heat treatment resulted in diffusion of magnesium and oxygen ions out of the ZrO_2 phase and promoted the formation of tetragonal and monoclinic ZrO_2. © 1997 Elsevier Science S.A.

Keywords: Defect structures; $MgO-Al_2O_3-ZrO_2$; Rapid solidification

1. Introduction

Magnesium aluminate spinel ($MgAl_2O_4$) has been the subject of numerous scientific analyses due to the unusually wide range of stoichiometries it can possess over a wide temperature range. With a melting point of 2105°C, spinel is also an excellent refractory ceramic but, unfortunately, has poor thermal shock characteristics. It has potential use as an RF heating window in fusion reactors as well as for special case shapes in the steel industry due to its excellent permanent liner change and permanent volume change. Fabrication of a composite of spinel with zirconia (ZrO_2) could produce a ZrO_2-toughened, high-strength structural ceramic. The most well-known example of a ZrO_2 composite is ZrO_2-toughened Al_2O_3, a structural ceramic in which the toughening is provided by ZrO_2 present in the tetragonal form (t-ZrO_2), normally stable at temperatures greater than about 1170°C [1–3]. Retention of this high-temperature polymorph at room temperature can be accomplished by several techniques, such as sol–gel processing and other chemical synthesis methods [4,5]. Rapid solidification (RS) is another technique in which ZrO_2 can be quenched directly into the t-ZrO_2 polymorph, resulting in a fine-grained microstructure. Rapid solidification of Al_2O_3–ZrO_2 binary systems has been well characterized [6–8] and the materials are used industrially as abrasives [9]. More significantly, it recently has been shown that a fine-grain size, dense, high-strength, high-toughness $Al_2O_3-ZrO_2$ composite can be fabricated from RS precursor powders [10].

Fig. 1 shows the ternary $Al_2O_3-MgO-ZrO_2$ phase diagram determined experimentally by Bierezhnoi and Kordyuk [11]. Two ternary eutectics and one binary pseudo-eutectic (along the $ZrO_2-MgAl_2O_4$ join) were identified, as shown on the diagram. Table 1 lists the compositions of the two ternary eutectics. One composition will be identified as Al_2O_3-rich (42.1 mol% Al_2O_3) and one will be identified as MgO-rich (42.1 mol% MgO). These two eutectics fall into compatibility trian-

* Corresponding author. Tel.: +1 619 5345425; fax: +1 619 5345698; e-mail: jmckittrick@ucsd.edu.

PII S0921-5093(97)00064-6

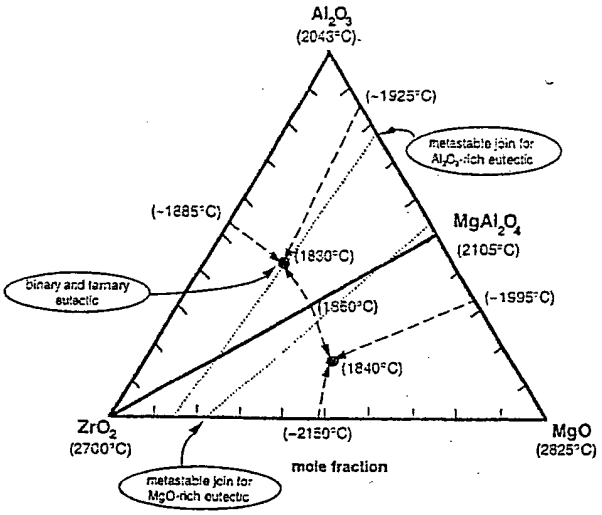

Fig. 1. The ternary Al_2O_3–MgO–ZrO_2 phase diagram [11].

gles which both have $MgAl_2O_4$ and ZrO_2 as end members. Fig. 2(a) and (b) shows the binary phase diagrams for ZrO_2–MgO [12] and MgO–Al_2O_3 [13], respectively. The ZrO_2–MgO phase diagram shows that the ZrO_2 cubic phase field (c-ZrO_2) extends up to approximately 21 mol% MgO at $T \sim 2100$°C. There is some confusion regarding the MgO–Al_2O_3 phase diagram in the Al_2O_3-rich portion. Some experimental work reports a eutectic between spinel and Al_2O_3 [14–17] while thermodynamic modeling identifies a peritectic [13]. The thermodynamic modeling of the MgO–Al_2O_3 phase diagram shows surprisingly good agreement between experiment and theory across the whole compositional field and the phase diagram is considered to be the most reliable. The spinel phase, $MgAl_2O_4$, displays a high degree of non-stoichiometry at $T \sim 2270$°C and can exist from 13.4 to 61.6 mol% MgO.

In this study, an extension of RS of the Al_2O_3–ZrO_2 system was directed to the ternary eutectics in the Al_2O_3–MgO–ZrO_2 system. Although quite a lot of research has been done on solid-state reactions in the binary systems (Al_2O_3–ZrO_2, ZrO_2–MgO, MgO–Al_2O_3), the ternary system has not been widely studied. A wide range of non-stoichiometric spinels has been found in rapid solidification of MgO–Al_2O_3 compositions [18] and significant variations in MgO content can be found in MgO-stabilized ZrO_2. No work has been done on RS in the MgO–ZrO_2 system or in the Al_2O_3–MgO–ZrO_2 system. It was the goal of this study to rapidly solidify the ternary eutectic compositions and study the as-quenched phases and the phase development during annealing.

2. Experimental techniques

Technical grade commercial powders of α-Al_2O_3, monoclinic ZrO_2 (m-ZrO_2) and MgO were mixed according to the two eutectic compositions shown in Table 1 and then pressed to form rods of about 6 cm length and 1 cm in diameter. The rods were heated to 1200°C for 2 h to produce a more structurally robust body. The rods were then suspended in a 5-cm diameter graphite susceptor above a twin roller solidification device and were inductively heated by an RF generator. Liquid droplets formed on the end of the rod and were allowed to drop between the rollers rotating with surface speeds of about 1.6 m s^{-1}. This apparatus is ideally suited to RS experiments on eutectic compositions: details of the experimental apparatus are reported elsewhere [19]. The quenched materials were in the shape of thin foils ranging from 50 to 1000 μm in thickness and from 0.25 to 2 cm in length, depending on the processing and roller conditions. The solidified foil thicknesses were measured with a micrometer to ±0.5 μm. X-ray diffraction (XRD) was performed on powders obtained from crushing the 500-μm-thick solidification product. For annealing experiments, the as-quenched 500-μm-thick foils were heat treated for 1 h at temperatures between 800 and 1600°C and then crushed for XRD measurements.

3. Experimental results and discussion

3.1. As-quenched materials

Fig. 3 shows the XRD pattern from the as-solidified Al_2O_3-rich eutectic. As shown, the peaks corresponding to the spinel phase and c-ZrO_2 do not match with the JCPDS standards due to the high concentration of MgO in ZrO_2 and low concentration in the spinel

Table 1
Compositions and melting temperatures of the two Al_2O_3–MgO–ZrO_2 ternary eutectics [11]

	Compositions						Melting temperature (°C)
	Al_2O_3		MgO		ZrO_2		
	mol%	wt.%	mol%	wt.%	mol%	wt.%	
Al_2O_3-rich	42.1	43	17.4	7	40.5	50	1830
MgO-rich	16.6	20	42.1	20	41.3	60	1840

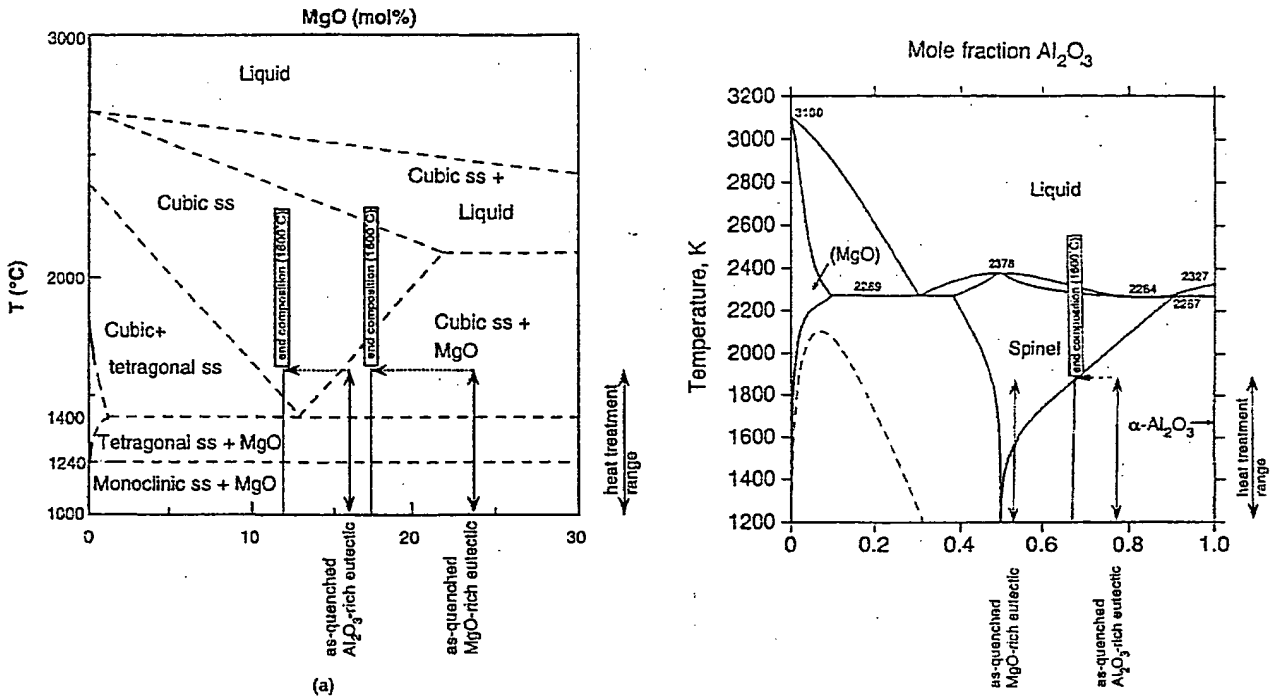

Fig. 2. Binary phase diagrams for (a) ZrO_2–MgO [12] and (b) Al_2O_3–MgO [13].

phase. The values of x in $Mg_xAl_{2(1-x)}O_{3-2x}$ ($0 \leqslant x \leqslant 0.5$, $x = C_{MgO}$ in spinel) and y in $Mg_yZr_{1-y}O_{2-y}$ ($0.1 \leqslant y \leqslant 0.25$, $y = C_{MgO}$ in ZrO_2) phases were determined by the lattice parameters calculated from the XRD data. For non-stoichiometric spinels, the composition is often written as $MgO \cdot n\ Al_2O_3$. In the present case, $x = 1/(n+1)$, which is the mole fraction of MgO in the spinel. The lattice parameters calculated from the four most intense diffraction lines for both the spinel and c-ZrO_2 phases were averaged. Spinel and c-ZrO_2 are cubic and the relationship between d-spacings and the lattice parameter (a) is $d_{hkl} = a/\sqrt{(h^2+k^2+l^2)}$.

For c-ZrO_2, the Aleksandrov et al. [20] equation was used:

$$a_z = \frac{4}{\sqrt{3}}\left[R_{Zr} + R_O + \frac{\Sigma_k (P_k M_k \Delta R_k)}{1 + \Sigma_k M_k (P_k - 1)}\right] \quad (1)$$

where a_z = c-ZrO_2 lattice parameter, R_{Zr}, R_O, R_k are the ionic radii of zirconium, oxygen and the k-th stabilizing element, P_k is the number of ions of each stabilizing element in the oxide molecule, M_k is the mole fraction of the stabilizing element and ΔR_k is the difference between ionic radii of zirconium and the stabilizing element. According to Eq. (1), as the amount of stabilizing element is increased, the lattice parameter of ZrO_2 decreases due to the substitution of smaller ions on the Zr^{4+} sites. It is assumed that a negligible amount of Al_2O_3 is dissolved in ZrO_2. Although it has been observed that in sol–gel-derived materials up to 40 mol% Al_2O_3 can be dissolved in ZrO_2 [21], this has not been observed in RS-derived materials [6–8]. The radius of Mg^{2+} in the ZrO_2 lattice was calculated to be 0.0648 nm by using the lattice parameters tabulated for MgO-stabilized c-ZrO_2 from other data [22]. Substituting into Eq. (1) using $P_k = 1$, $r_{Zr} = 0.0824$ nm and $r_O = 0.1400$ nm, the lattice parameter (a_z) as a function of mole fraction of MgO (y) is:

$$a_z\ (\text{nm}) = 0.5136 - 0.0407y \quad (2)$$

Chiang and Kingery [23] have determined the lattice parameter (a_s) of magnesium aluminate spinel ($Mg_xAl_{2(1-x)}O_{3-2x}$) as a function of MgO mole fraction, x:

$$a_s\ (\text{nm}) = 0.7848 + 0.0470x \quad (3)$$

for MgO fractions from 0.20 to 0.50. The decrease of the spinel lattice parameter with increasing Al_2O_3 content is due to the creation of vacancies on the cation sublattice and to the substitution of the smaller Al^{3+} for the larger Mg^{2+}. In Ref. [23], it is possible that there was a depletion of magnesium in the samples, which would shift what was considered the stoichiometric spinel lattice parameter to a higher value, but da_s/dx should remain the same. In fact, the slope found in this experiment is identical to the one found by Sarjeant and Roy [18] for splat-quenched compositions of magnesium aluminate spinels.

Table 2 lists the XRD results for the as-quenched materials. For the Al_2O_3-rich eutectic, under equilibrium conditions the phase assemblage should be $Al_2O_3 + MgAl_2O_4 + ZrO_2$. However, in the RS, materials nucleation of the Al_2O_3 primary phase was sup-

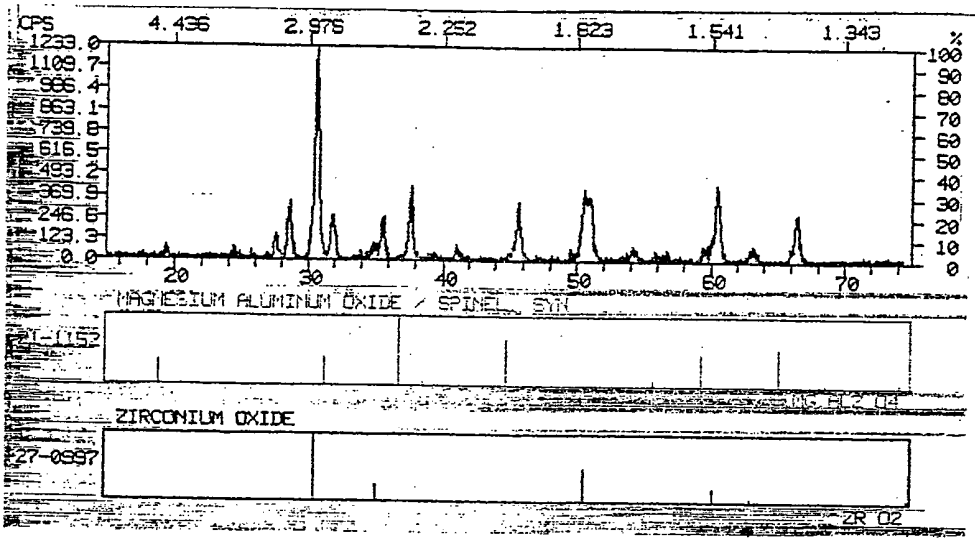

Fig. 3. X-ray diffraction pattern of the as-quenched Al_2O_3-rich eutectic composition in comparison with the JCPDS standards for $MgAl_2O_4$ and c-ZrO_2.

pressed and an Al_2O_3-rich spinel ($x = 0.221$) and monoclinic (m) + c-ZrO_2 ($y = 0.155$) were found. The absence of one primary phase in the Al_2O_3-rich system indicates that surface energy constraints limit the nucleation of that phase to decrease the total interphase boundary energy. It is not surprising that α-Al_2O_3 formation is suppressed due to the lattice mismatch with the two other cubic phases. Fig. 4 shows a transmission electron micrograph (TEM) micrograph of the as-quenched Al_2O_3-rich composition. The characteristic lamellar structure of a solidified eutectic is seen. There are only two phases observed; the light phase is the Al_2O_3-rich spinel and the dark phase is ZrO_2.

The presence of m-ZrO_2 ($\sim 10\%$) in the Al_2O_3-rich composition can be explained by MgO vaporization from the surface of the liquid, and not from incomplete melting. If MgO vaporization occurred with simultaneous partial nucleation of unstabilized c-ZrO_2 (the high-temperature polymorph) on the surface of the droplet during melting, m-ZrO_2 would form after cooling to ambient temperature (see Fig. 2(a)). It has been shown in other works that substantial evaporation of MgO from ZrO_2 occurs at elevated temperatures [24,25] and is what likely occurred in the present case.

Table 2
Summary of the X-ray diffraction results on the as-quenched crystalline materials produced by twin rolling

Composition (mol%)	Phases present (mol% MgO)
42.1Al_2O_3–17.4MgO–40.5ZrO_2 (Al_2O_3-rich)	Spinel (22.1), m+c–ZrO_2 (15.5)
16.6Al_2O_3–42.1MgO–41.3ZrO_2 (MgO-rich)	Spinel (46.2), c-ZrO_2 (22.2), MgO

For the MgO-rich composition under equilibrium conditions, the phase assemblage should yield MgO + $MgAl_2O_4$ + ZrO_2. In the RS material, a slightly Al_2O_3-rich spinel phase ($x = 0.462$), MgO and c-ZrO_2 ($y = 0.222$) were found. Because of the high MgO content in the starting composition, m-ZrO_2 was not found, strengthening the argument that some MgO vaporization occurred during the melting and solidification experiment and the presence of m-ZrO_2 is not a by-product of partial melting.

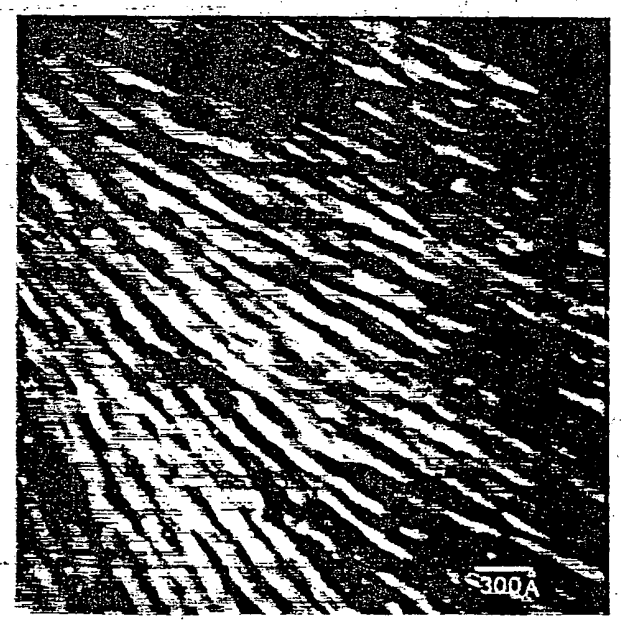

Fig. 4. TEM micrograph of the as-quenched Al_2O_3-rich eutectic. The light phase is the MgO-depleted spinel and the dark phase is c-ZrO_2.

Table 3
Molar phase contents of the rapidly solidified (RS) compositions compared with the equilibrium (Ξ) mixtures (determined from the phase diagram given in Fig. 1)

	Spinel (mol%)		ZrO_2 (mol%)		Al_2O_3 (mol%)		MgO (mol%)	
	Ξ	RS	Ξ	RS	Ξ	RS	Ξ	RS
Al_2O_3-rich	21.1	53.2	49.0	46.8	29.9	0	—	—
MgO-rich	19.9	30.8	49.5	53.1	—	—	30.6	16.1

Fig. 1 shows the compatibility relationships for the as-quenched phases. For the Al_2O_3-rich composition, the two end phases (Al_2O_3-rich spinel and c-ZrO_2) are connected by a metastable join containing a binary eutectic which has the same composition as the ternary eutectic. For the MgO-rich composition, the metastable compatibility triangle houses the ternary eutectic. The MgO-rich eutectic phase assemblage has a smaller fraction of the pure MgO phase with the balance incorporated into the c-ZrO_2 phase. It is interesting to note that even an excess of MgO does not promote the formation of a stoichiometric or an MgO-rich spinel. Table 3 lists the molar percentages of each phase in the RS material and are compared with what would be obtained under equilibrium conditions. For the Al_2O_3-rich composition, a higher fraction of spinel is found because all of the Al_2O_3 is dissolved in it: there is no pure Al_2O_3 phase. For the MgO-rich composition, a higher fraction of spinel and c-ZrO_2 is found due to the high concentration of MgO in each phase. The amount of the MgO phase is decreased from 30.6 mol% (under equilibrium conditions) to 16.1 mol% for the RS material.

It appears that significant supersaturation of MgO in ZrO_2 cannot occur through rapid solidification in these compositions. As seen in the binary phase diagram (Fig. 2(a)), c-ZrO_2 coexists with MgO in a compositional range of at least 12 mol% MgO at $T \geqslant 1400$°C. During RS, it could be possible to suppress the nucleation of the MgO phase and thereby enrich the spinel and c-ZrO_2 with MgO. Assuming that even in the unlikely case that $x = 0.6$ (the maximum MgO content in spinel according to the equilibrium phase diagram), to maintain a mass balance this would require that $y = 0.30$, which roughly corresponds to the compound $Mg_2Zr_5O_{12}$. There was no experimental evidence found for this phase and, because of the presence of the MgO phase, indicates that supersaturation of MgO in ZrO_2 does not occur under RS conditions.

The spinel and c-ZrO_2 phases in both eutectics compete for MgO during the solidification process. In the Al_2O_3-rich eutectic, close to the minimum amount of MgO is dissolved in the spinel and ZrO_2 phases to maintain a spinel and c-ZrO_2 structure. The presence of ZrO_2 has been found to lead to an increase in solubility of MgO in Al_2O_3 and that MgO preferentially dissolves in Al_2O_3 over that of ZrO_2 [26]. In the MgO-rich composition, close to the maximum amount of MgO is dissolved in the ZrO_2 and spinel phases, with the balance present as pure MgO.

3.2. Annealing experiments

Table 4 lists the phase development of the two ternary eutectics as a function of annealing temperature for 1-h anneals. For the Al_2O_3-rich composition, the Al_2O_3-rich spinel phase is present along with m + c-ZrO_2 at 800°C. Nucleation of γ-Al_2O_3 occurred in samples held at 1000°C. The γ-polymorph is a cubic polymorph with a spinel structure and the lattice parameter exactly matches that of the Al_2O_3-rich spinel. In previous work on rapidly solidified MgO–Al_2O_3 compositions, the γ-phase was found for Al_2O_3-rich compositions [18]. There is an anomaly in the RS spinel phase development during annealing compared with annealing single crystals or polycrystalline Al_2O_3-rich spinels. In single crystals ($x = 0.125$–0.5), it was reported that precipitation of Al_2O_3 occurs first by the nucleation of 10-nm crystallites, then by the formation of a platy monoclinic phase ($x = 0.06$) and finally the precipitation of α-Al_2O_3 [27–29]. No γ-Al_2O_3 was

Table 4
Summary of the results for the annealed RS Al_2O_3–MgO–ZrO_2 ternary eutectics

Composition	Annealing conditions (1 h)	Phases present
17.4MgO–42.1Al_2O_3 –40.5ZrO_2 (Al_2O_3-rich)	800°C	Spinel + m + c-ZrO_2
	1000–1200°C	Spinel + γ-Al_2O_3, m + c–ZrO_2
	1400–1600°C	Spinel, γ + α-Al_2O_3, m + t + c-ZrO_2
42.1MgO–16.6Al_2O_3 –41.3ZrO_2 (MgO-rich)	800–1000°C	Spinel + MgO + c-ZrO_2
	1600°C	Spinel + MgO, m + t + c–ZrO_2

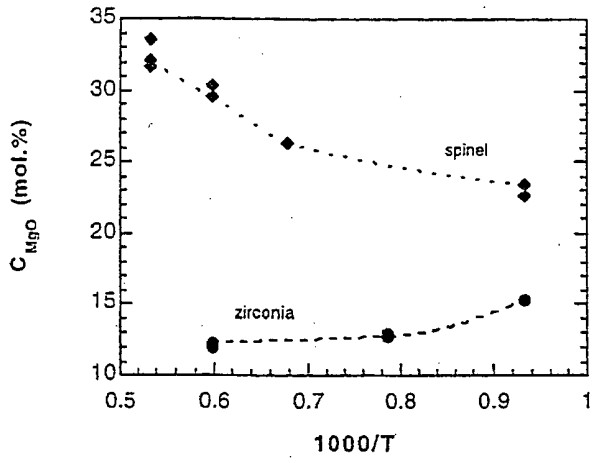

Fig. 5. Concentration of MgO in the spinel phase ($C_{MgO} = x$) and in c-ZrO_2 ($C_{MgO} = y$) as a function of annealing temperature.

found. In the work on the polycrystalline spinels ($x = 0.333$), it was found that α-Al_2O_3 directly precipitates from the spinel and again no γ-Al_2O_3 was reported at $T \geqslant 1400$°C [30]. In the present study, nucleation of γ-Al_2O_3 initially occurred and α-Al_2O_3 was found after annealing at 1400°C. In the polycrystalline work, the x-value was closer to stoichiometry whereas in the present work, x ranged from 0.221 to 0.340. It is also possible that the presence of c-ZrO_2 may have suppressed the nucleation of α-Al_2O_3, since it was reported in the polycrystalline work that α-Al_2O_3 nucleates on the surface of spinel. t-ZrO_2 was detected only under anneals at $T > 1400$°C. This is consistent with the phase diagram which reports the eutectoid decomposition (c-$ZrO_2 \rightarrow$ t-ZrO_2 + MgO) temperature at 1400°C.

Fig. 5 plots the concentration of MgO in the spinel phase and in c-ZrO_2 as a function of reciprocal temperature as determined from Eqs. (1) and (2). As shown, the MgO concentration increased in the spinel phase (from $x = 0.221$ to $x = 0.340$) and decreased in the ZrO_2 phase (from $y = 0.155$ to $y = 0.116$) as the temperature was raised. The MgO content increased in the spinel due to two factors: the nucleation of γ-Al_2O_3 and to a lesser extent to the MgO diffusion from c-ZrO_2 into the spinel phase. Diffusion of MgO from c-ZrO_2 resulted in the formation of t-ZrO_2, in accordance with the phase diagram. Fig. 2(b) pictorially shows the change in composition of the spinel after annealing the as-quenched material at 1600°C. The phase development during annealing follows what is predicted from the phase diagram, namely that an alumina phase will nucleate and co-exist with a spinel phase.

The fraction of m-ZrO_2 (f_m) is found from the XRD results by the ratio of the (111) and ($\bar{1}11$) peak intensities for the three polymorphs:

$$f_m = \frac{I_m(111) + I_m(\bar{1}11)}{I_m(111) + I_m(\bar{1}11) + I_t(111) + I_c(111)} \quad (4)$$

where I_m, I_c and I_t are the intensities of the 100% (111) or peaks. The fraction of m-ZrO_2 as a function of annealing temperature is plotted in Fig. 6. As shown, a small fraction of m-ZrO_2 is initially present, as discussed earlier. The amount does not change appreciably until the temperature is equal to or greater than 1200°C, where f_m increases and reaches about 0.8 at 1600°C. The t-ZrO_2 can subsequently transform to m-ZrO_2 from cooling if the grain size is large enough or from the stress induced t → m transformation is produced from crushing the sample for powder X-ray work. Fig. 2(a) shows pictorially the compositional change after annealing at 1600°C. The as-quenched material composition falls in the c-ZrO_2 + MgO phase field and after annealing falls in the c-ZrO_2 field. However, upon cooling it is predicted that t + m-ZrO_2 will form.

For the heat-treated MgO-rich eutectic, spinel, MgO and c-ZrO_2 phases co-exist over a large temperature range for various annealing times. Only in samples held at 1600°C for is the presence of m + t-ZrO_2 detected along with c-ZrO_2. Fig. 7 shows the data from the annealing experiments on the MgO-rich eutectic. As shown, the MgO content in the spinel remains constant within experimental error over the annealing temperature range while the c-ZrO_2 shows a marked decrease in MgO concentration with increasing annealing temperature. No γ-Al_2O_3 or α-Al_2O_3 was found under any annealing condition. This is in agreement with the results of Saalfeld and Jagodzinski [27,28] in which precipitation of an Al_2O_3 phase did not occur for slightly Al_2O_3-rich spinels. The MgO diffuses out of the c-ZrO_2 phase and into the MgO phase in accordance with the phase diagram. It has been shown that the eutectoid reaction c-$ZrO_2 \rightarrow$ m-ZrO_2 + MgO occurs for $T \leqslant 1240$°C in a compositional range $x = 0.081 \rightarrow 0.186$ [31]. Although in the present work, m-ZrO_2 was not

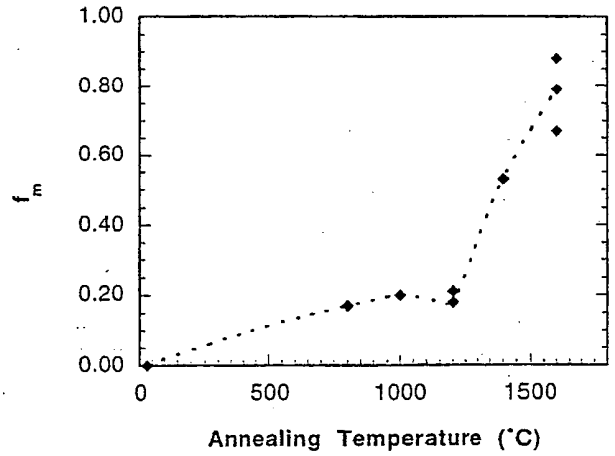

Fig. 6. Fraction of m-ZrO_2 as a function of annealing temperature in the Al_2O_3-rich eutectic.

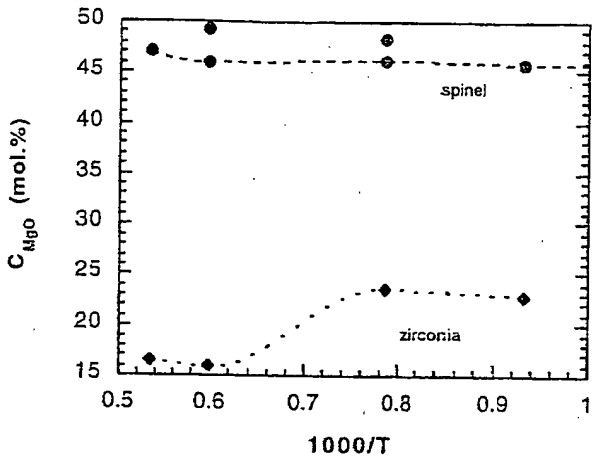

Fig. 7. Concentration of MgO in the spinel phase ($C_{MgO} = x$) and in c-ZrO_2 ($C_{MgO} = y$) as a function of heat-treatment temperature for the MgO-rich eutectic.

found at the low-temperature anneals, it may be due to the short annealing time coupled with the presence of the cubic spinel phase. Fig. 2(a) pictorially shows the compositional change of the zirconia phase after annealing at 1600°C. The starting composition falls in the c-ZrO_2 + MgO phase field and remains there after annealing. The t + m-ZrO_2 nucleate upon cooling from the high temperature.

For the spinel phase, the calculated as-quenched composition ($x = 0.462$) is nearly the stoichiometric one; however, as indicated earlier, there is uncertainty as to the exact lattice parameter of stoichiometric spinel in this work. It is assumed that during annealing at high enough temperatures, the spinel composition would go to equilibrium and maintain a stoichiometric composition. Starting with 46.2 mol% MgO, a change of 3.8 mol% would yield a difference in lattice parameter of 0.0019 nm, which is a measurable amount by X-ray diffraction. Since this was not measured, it is possible that the as-quenched composition was closer to the stoichiometric one.

4. Conclusions

Rapid solidification resulted in diverse compositional and structural phase assemblages in MgO–Al_2O_3–ZrO_2 eutectics. In the Al_2O_3-rich eutectic, rapid solidification resulted in the suppression of the primary Al_2O_3 phase and the formation of an Al_2O_3-rich spinel (22.1 mol% MgO) and c-ZrO_2 (15.5 mol% MgO). The characteristic lamellar microstructure of eutectics was observed. A metastable binary eutectic was found between these two phases and had the same composition as the ternary eutectic. Annealing these materials resulted in the formation of γ-Al_2O_3 which grew by depleting the Al_2O_3-rich spinel of Al_2O_3. After annealing at 1600°C for 1 h, the MgO content in the spinel increased to 34 mol% and α-Al_2O_3 was detected. The composition of the spinel changes due to two factors: nucleation of γ-Al_2O_3 and to a lesser extent diffusion of MgO out of the c-ZrO_2. The MgO concentration in the zirconia decreased to 11.6 mol%.

For the MgO-rich ternary eutectic, rapid solidification yielded a three-phase assemblage of MgO, a nearly stoichiometric spinel (46.2 mol% MgO) and c-ZrO_2 (22.2 mol% MgO). Annealing these materials results in the growth of the MgO phase from diffusion of MgO out of c-ZrO_2. The spinel composition did not change significantly. Depletion of MgO from the c-ZrO_2 results in the eventual formation of t-ZrO_2, but only after annealing at 1600°C.

References

[1] A.G. Evans, in N. Claussen, M. Rühle and A.H. Heuer (Eds.), *Science and Technology of Zirconia, Advances in Ceramics*, Vol. 12, American Ceramic Society, Columbus, OH, 1984, pp. 193–212.
[2] A.G. Evans and A.H. Heuer, *J. Am. Ceram. Soc., 63* (5–6) (1980) 241.
[3] N. Claussen, *J. Am. Ceram. Soc., 59* (1–2) (1976) 49.
[4] B.H. Davis, *Commun. Am. Ceram. Soc., 67* (8) (1984) C-168.
[5] B. Fegley, Jr., P. White and H.K. Bowen, *Commun. Am. Ceram. Soc., 68* (2) (1985) C60.
[6] N. Claussen, G. Lindemann and G. Petzow, *Ceram. Int., 9* (3) (1983) 83.
[7] J. McKittrick, G. Kalonji and T. Ando, in S. Somiya, N. Yamamoto and H. Yanagida (Eds.), *Science and Technology of Zirconia, Advances in Ceramics*, Vol. 24, American Ceramic Society, Columbus, OH, 1988, pp. 267–275.
[8] V. Jayaram, C.G. Levi, T. Whitney and R. Mehrabian, *Mater. Sci. Eng., A124* (1990) 65.
[9] J.W. Poole, M.C. Flemings, T. Gaspar and M. Simpson, *US Patent 4917852* (Apr. 17, 1990).
[10] J. Freim and J. McKittrick, *J. Am. Ceram. Soc.*, submitted.
[11] A.S. Bierezhnoi and R.A. Kordyuk, *Dopovidi Akad. Nauk Ukr. RSR. 4* (1964) 506.
[12] C.F. Grain, *J. Am. Ceram. Soc., 50* (6) (1967) 288.
[13] B. Hallstedt, *J. Am. Ceram. Soc., 75* (6) (1992) 1497.
[14] D. Viechnicki, F. Schmid and J.W. McCauley, *J. Am. Ceram. Soc., 57* (1) (1974) 47.
[15] A.M. Alper, R.N. McNally, P.H. Ribbe and R.C. Doman, *J. Am. Ceram. Soc., 45* (6) (1962) 263.
[16] D.M. Roy, R. Roy and E.F. Osborn, *J. Am. Ceram. Soc., 36* (1953) 149.
[17] G.A. Rankin and H.E. Merwin, *J. Am. Ceram. Soc., 38* (3) (1916) 568.
[18] P.T. Sarjeant and R. Roy, *J. Appl. Phys., 38* (1967) 4540.
[19] J. McKittrick, *Ph.D Thesis*, Dept. of Materials Science and Engineering, MIT, Cambridge, MA, 1988.
[20] V.I. Aleksandrov, G.E. Val'yano, B.V. Lukin, V.V. Osiko, A.E. Rautbort, V.M. Tatarintsev and V.N. Filatova, *Izves. Akad. Nauk SSSr (Neorg. Mat.), 12* (2) (1976) 273.
[21] M.L. Balmer, F.F. Lange and C.G. Levi, *J. Am. Ceram. Soc., 77* (8) (1994) 2069.
[22] S.M. Sim and V. Stubican, *J. Am. Ceram. Soc., 70* (7) (1987) 521.

[23] Y.-M. Chiang and W.D. Kingery, *J. Am. Ceram. Soc., 72* (2) (1989) 271.
[24] P.A. Tikhonov, A.K. Kuznetsov and E.K. Keler, *Inorg. Mater., 7* (11) (1971) 1794 (English translation).
[25] Y. Sakka, Y. Oishi and K. Ando, *J. Am. Ceram. Soc., 69* (2) (1986) 111.
[26] T. Kosmač, J.S. Wallace and N. Claussen, *Commun. Am. Ceram. Soc., 64* (5) (1982) C66.
[27] H. Saalfeld and H. Jagodzinski, *Z. Kristallogr., 110* (1958) 197.
[28] H. Saalfeld and H. Jagodzinski, *Z. Kristallogr., 109* (1957) 87 (in German).
[29] H. Saalfeld, *Z. Kristallogr., 109* (1957) 388 (in German).
[30] P.C. Panda and R. Raj, *J. Am. Ceram. Soc., 69* (5) (1986) 365.
[31] S.C. Farmer, A.H. Heuer and R.H.J. Hannink, *J. Am. Ceram. Soc., 70* (6) (1987) 431.